6G automatic modulation classification using deep learning models in the presence of channel noise, CFO, and PN

Zhraa Zuheir Yahya[1] , Dia M. Ali[1,*] , Marwa Y. Abdallah[2]

[1]*Department of Communication Engineering, College of Electronics Engineering, Ninevah University, Ninevah, Iraq.*
[2]*Techniques Engineering Department, Technical Engineering College, Northern Technical University, Ninevah, Iraq.*

*****Corresponding author:** dia.ali@uoninevah.edu.iq

Abstract:

An efficient and remarkable automatic modulation classification (AMC) technique is essential with the advent of sixth-generation (6G) communication systems. Using the pre-trained convolutional neural network (CNN), a deep learning (DL) approach to classify eight types of digital modulated signals. National Instrument LabVIEW NXG is used to build the modulation transceivers at 100 GHz, a 6G carrier frequency. The dataset was collected in a complicated environment, including carrier frequency offset (CFO), phase noise (PN), and distinct signal-to-noise ratios (SNR). Through experimental simulation, an improvement in the classification accuracies was achieved. In particular, the outstanding accuracy rates achieved are 98.68% and 96.05% using ResNet18 and ResNet101, respectively. Furthermore, these models can classify the modulated signals at lower SNRs. These innovative models are suitable and effective to utilize for 6G wireless communication networks.

1. Introduction

Advanced evolution in technologies is in progress for sixth-generation (6G) communication networks for high-speed data communication and increased connectivity. Sub-THz frequency bands are expected to be employed in the 6G systems. These frequencies allow higher modulation order utilization and achieve higher bandwidth efficiencies. These cutting-edge technologies increase the complexity of the received signals. Automatic modulation classification (AMC) is a technique used for interference recognition and signal detection in both cooperative and non-cooperative systems. This technique can recognize the modulation type of the received signals without the need to know the system parameters. Likelihood and feature-based extraction are two common types of AMC techniques, where the first one requires a large amount of computation, and the second depends on the specialists. Therefore, these two approaches are insufficient for complicated communication systems. Sophisticated AMC approaches are required to detect the

modulated signals even in the existence of the carrier frequency offset (CFO) and phase noise (PN). Doppler shift and the inconsistency between the transceiver's oscillators cause CFO, which in turn will induce a rotation on the received constellation diagram with a specific angle. Meanwhile, the PN reduces the signal-to-noise ratio (SNR) and rotates the received constellation points around the reference point [1, 2].

Recently, Deep learning (DL) has become prominent as a technology in a variety of disciplines. In this context, DL is widely employed to tackle complicated environmental issues and enhance the efficiency of wireless systems. DL-based modulation classification has the capability to recognize signal properties without requiring expert knowledge, which is the case with conventional techniques. Convolutional neural network (CNN) is one of the most widespread and effective DL models, which consists of several convolutional, pooling, and fully connected layers. The convolutional layer is essential to recognize different features introduced in the input dataset. After the convolution, the pool-

ing layer decreases the dimensionality of the obtained features, speeding up computational processes. Afterward, the completely connected layer then combines the previously separated local features into comprehensive global features, eventually leading to classification based on these distinct aspects. Consequently, to understand the nature of the modulated signals, a transformation is employed to render the signal into a two-dimensional representation resembling constellation and time-frequency diagrams. Subsequently, the convolutional layers become operational, skilfully extracting intricate features inherent in the image-form signal, enabling classification using the fully connected layer [2–7].

DL-based AMC has better durability than conventional AMC approaches and higher classification accuracies. However, in the case of small samples, the DL models may not perform well. To solve this problem, data quality improvement and transfer learning models are required [7].

The remainder of this paper is organized as follows: Section 2 presents the literature review, section 3 describes the methodology of this work, and Section 4 shows the obtained results and discussion. Finally, the conclusion is in section 5.

2. Literature review

In recent years, there has been a large increase in the use of DL in AMC, which processes baseband signals intelligently and automatically extracts valuable features [8, 9].

In [10], CNN was used to classify modulation techniques in an orthogonal frequency division multiplexing (OFDM) system, which also involved carrier phase offset (PO). The proposed approach improves accuracy by eliminating the PO. The multi-scale network is used in [11] to introduce a distinctive AMC method. This method learns discriminative and separable features through a novel loss function combining the center and cross-entropy losses. Compared to benchmark methods, their suggested approach yields higher classification accuracy. The authors in [12] used a combination of ResNet and long short-term memory (LSTM) algorithms for AMC. Except for 64-quadrature amplitude modulation (64-QAM) and WBFM, their proposed method achieved a classification accuracy exceeding 98% in most modulation schemes. For extracting the Inphase/Quadrature (IQ) signal and multi-channel constellation features, the authors of [13] built a CNN with a double-branch architecture and exhibited multi-feature fusion. The proposed model has a recognition rate of 90% to 95%. The identification accuracy of the CNN decreases by at least 15% when the highest frequency offset increases from 25 to 100 kHz. However, the suggested technique only experiences a 6% decrease.

In [14], the authors proposed using a DR2D preprocessing technique to obtain distinctive modulation features. Concurrently, they developed a DenseNet feature extraction network, implementing early fusion to distinguish and differentiate the acquired features. The results of their simulations demonstrate that the combination of DenseNet-F22 and the DR2D preprocessing approach constantly achieves an average classification accuracy exceeding 90%, with accuracy surpassing 60%. Notably, these impressive results

are consistently demonstrated in scenarios with SNRs exceeding 14 dB. A semi-supervised automatic modulation recognition model is proposed in [15] to achieve cross-domain classification. This model can adapt to different SNR domains without requiring training on labeled data for that specific domain. According to their findings, the suggested method outperforms conventional methods by 1% to 27%. In our previous study [16], the digital modulation transceivers were designed using LabVIEW NXG and implemented using software-defined radio (SDR) technology to collect practical datasets at three microwave frequencies. Three pre-trained CNN algorithms were used for AMC. The accuracies achieved were 94.64%, 92.86%, and 96.43% using MobileNet-V2, ResNet50, and ResNet18, respectively. AMC is presented by the authors in [17] as a lightweight ensemble model including convolutional, LSTM, and gated recurrent unit (GRU) layers. This innovative approach is referred to as a deep recurrent convolutional network, enhanced by the addition of an extra gated layer. The results of their meticulously conducted simulations demonstrate that the proposed solution achieves a remarkable 7% improvement in accuracy compared to existing models. The authors in [18] proposed a threshold denoising recurrent neural network for modulation categorization in 6G networks. The model was tested on several modulation schemes and SNR. The simulation results demonstrate that the suggested method outperforms existing methods in accuracy, speed, and computational complexity.

In [19], KD-GoogLeNet and Squeeze-Excitation (KD-GSENET) are used for AMC to mitigate noise mismatch issues. To improve the performance, the complex signals are transformed into colored images using a K-dimensional tree. The results show that the utilized method outperforms other conventional methods. The authors in [20] used combinatorial deep learning models for AMC. ConvLSTM and transformer block neural networks are used for classification at both lower and higher SNRs. Their results show that 66% classification accuracy is achieved at lower SNR and 93.5% at higher SNR.

In [21], the authors proposed a scalable AMC model that enables adaptability for new modulations and various signal specifications. The proposed model using meta-transformer-based few-shot learning outperforms other existing techniques at different SNRs. In [22], the authors used two distinct architectures of CNN models for AMC. Their results achieved classification accuracy of 53.65% using the first CNN and 94.39% using the second CNN.

In this study, CNN algorithms have been used for AMC. Various transceiver modulation schemes have been constructed using the LabVIEW NXG communication platform to collect datasets. The modulated signals transmitted through a wireless channel cause distortion at the receiver due to the CFO, PN, and Gaussian noise. Finally, the received constellation points are processed using pre-trained CNN models.

3. Methodology

This work has been accomplished in two phases. The first phase involved constructing modulator signal transceivers

and collecting datasets, while the second phase focused on training the dataset using pre-trained CNN networks. The entire process is illustrated in Fig. 1.

3.1 Signal model

Using NI LabVIEW NXG, the transmitter is designed to accommodate a range of modulation schemes, including 4-amplitude shift keying (4-ASK), 4-QAM, 16-phase shift keying (16-PSK), 16-QAM, 32-QAM, 64-QAM, 256-QAM, and 512-QAM. The block diagram of the proposed transceiver using LabVIEW NXG is illustrated in Fig. 2. The MT Generate Bits (Galois, PN Order) node was used to generate the bit sequences. An MT Generate QAM system parameter was used to calculate the QAM parameters. The node accepts an M-ary value that specifies a predefined symbol map with the number of distinct symbol map values to use as symbols. The out parameters and generated bits are entered into the modulator. Subsequently, the modulated signals are up-converted to 100 GHz (proposed for 6G networks) and then transmitted through a noisy wireless channel. This channel introduces the CFO and PN to the received signals. The received signals $y(t)$ are represented as follows:

$$y(t) = x(t) + n(t) \qquad (1)$$

where $n(t)$ is the additive noise. The noiseless signal for disrupted communication channels is expressed as

$$x(t) = e^{j(2\pi f_0 + \theta(t))} \sum_{-\infty}^{\infty} x(n)h(t) \qquad (2)$$

where f_0 is the CFO, and $\theta(t)$ is the PN; $h(t)$ is the impulse response of the channel.

After receiving the modulated signals, the two-dimensional data of constellation diagrams (IQ) are directly obtained from LabVIEW. Each image in the dataset contains random values of CFO and PN induced due to the wireless channel in addition to noise, as shown in Fig. 3. Finally, the collected constellation diagrams are prepared for training using CNN algorithms.

3.2 Training the dataset using CNN

The transfer learning method has been employed to classify the acquired constellation points at different SNRs using pre-trained CNN algorithms. ResNet18 and ResNet101 pre-trained CNNs are used for AMC. ResNet18 and ResNet101 are commonly utilized in practical and experimental approaches for many reasons that make them attractive over other models due to the ability to overcome the vanishing gradient issue, where these models use a residual network architecture that permits information to proceed through the network using residual connections. These connections enable the preservation of the information throughout the deep layer. In addition, ease of training, where due to the residual connections, ResNet models like ResNet101 can be trained without difficulties even at very deep. The ResNet models also have scalability modifiability and outstanding performance in image recognition.

3.2.1 ResNet18

ResNet18 is a pre-trained CNN with 71 layers and 78 connections. The size of the input images to be processed in this network is 227 × 227, and ResNet18 can recognize 1000 images. The image input layer of this network has been modified to accommodate the new image input with an input image size of 395 × 296 × 3 for RGB constellation
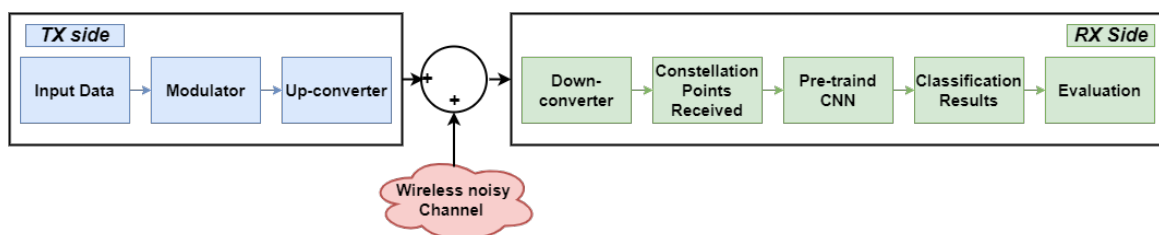

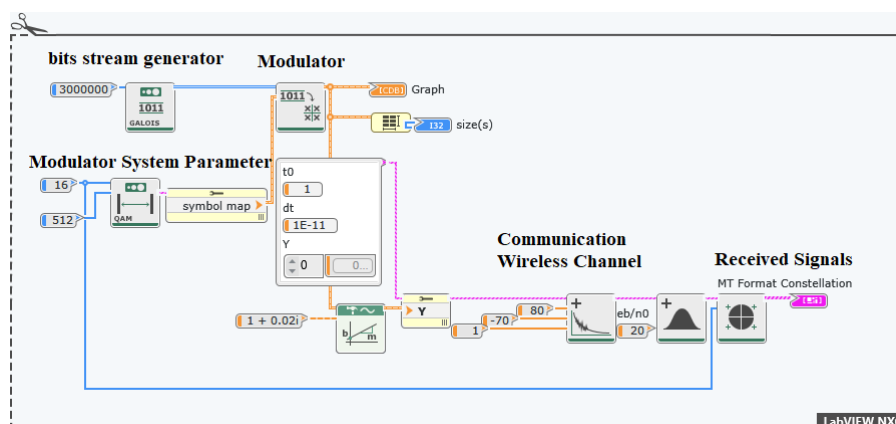**Figure 1.** Proposed transceiver block diagram.

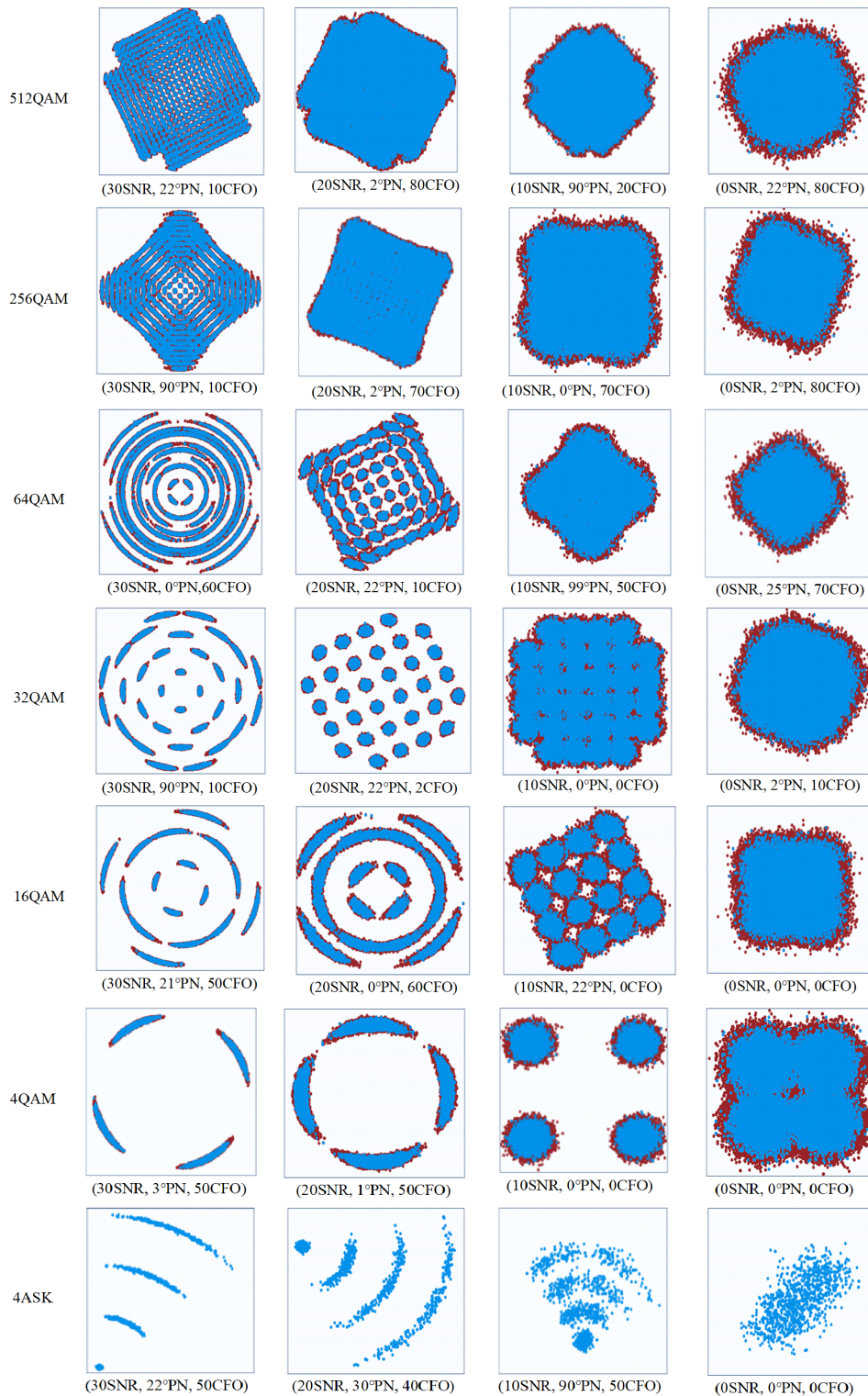**Figure 2.** LabVIEW NXG suggested a transceiver scheme.

Figure 3. Various snapshots of the received constellation diagram at various CFOs, PNs, and SNRs.

diagram images. The fully connected softmax and output classification layers have been changed to the new layer to recognize the eight modulation types.

3.2.2 ResNet101

ResNet101 is a pre-trained CNN with 347 layers and 379 connections. The size of the input images to be processed in this network is 224 × 224, and ResNet101 can recognize

1000 images. The image input layer of this network has been altered to accommodate the new image input with an input image size of 395 × 296 × 3 for RGB constellation diagram images. The fully connected softmax and output classification layers have been changed to the new layer to recognize the eight modulation types. The process of transfer learning is illustrated in Fig. 4.

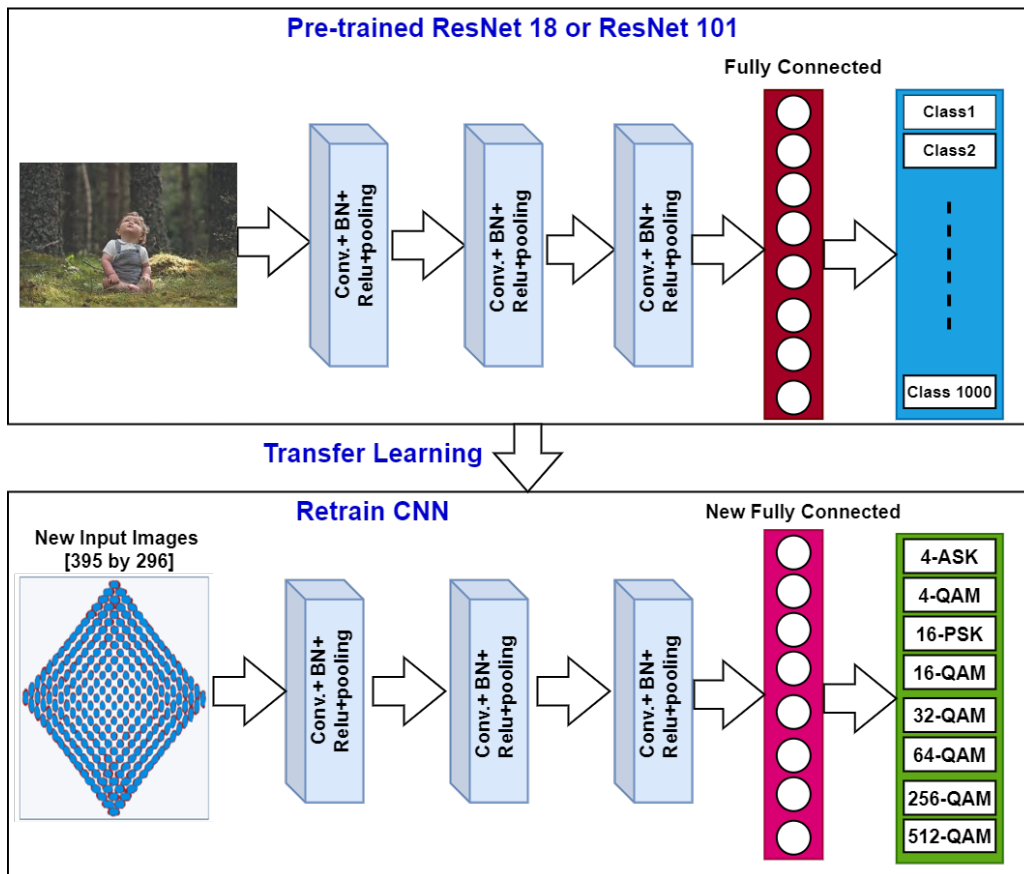The training parameters are listed in Table 1. To get ade-

Figure 4. Transfer learning process.

Table 1. CNN hyperparameters.

Parameter	Setting
Optimize algorithm	SGDM
Execution environment	GPU and CPU
Initial learn rate	0.01
Minibatch size	20, 12
Shuffle	Every epoch
Validation frequency	35
Maximum iteration	120
Iteration per epoch	4
Learn rate drop factor	0.1
Learn rate drop factor	10

quate performance, the minibatch size is picked to match the structure of each network, where the lower values slow down the training process. As for the initial learning rate, a compromised value is picked to achieve an acceptable performance. The higher values speed up the training process, with unstable performance, while the lower values slow down the training process. As a consequence, an initial learning rate value of 0.01 was picked up, which is compatible with both networks and provides satisfactory results in terms of accuracy. The optimized algorithm "SGDM" enhances the speed to the global minimum error using momentum, which increases gradient descent and reduces oscillations. The execution environment "GPU" accelerates the training by handling parallel computations, while the

CPU is less efficient and used for initial training and testing. Shuffling data every epoch enhances learning and reduces the probability of continuing to a particular sequence, which induces a more effective model. Evaluating the model on a regular basis, "35" at a specific number of iterations, "120," can observe performance on the validation set, avoid overfitting, and guarantee training ends at an adequate point. The learn rate drop factor was picked up to 0.1, which enhances the final accuracy once it is close to optimal performance. The period of learning rate factor drop was picked up to 10, which means minimizing the learning rate at every ten iterations boosts the training progress.

4. Results and discussion

This section discusses the simulation results of the 6G AMC model using pre-trained CNN algorithms and performance comparison with previous studies. According to the signal model, the dataset of size 1000 case was obtained from NI LabVIEW NXG for eight distinct modulation types named 4-ASK, 4-QAM, 16-PSK, 16-QAM, 32-QAM, 64-QAM, 256-QAM, and 512-QAM. The constellation diagram dataset has been trained and tested with a wide range of SNRs (-20 to 30 dB), various PN angles, and CFOs. The simulations have been performed with Matlab R2020b and a computing system with an Intel(R) Core(TM) i7-8550U CPU @ 1.80 GHz, 1.99 GHz, and 8.00 GB Ram. Each model underwent simulation within a setting employing minibatch sizes of 20 and encompassing 12 training cycles.

An early interrupt mechanism was employed to counteract overfitting. Additionally, validation checks were conducted every 35 cycles, while the maximum epoch limit was capped at 30.

The time that ResNet18 took to train the dataset was 3 minutes and 11 seconds, while in ResNet101, the training time was 4 minutes and 17 seconds. As for the test time, both ResNet18 and Resnet101 took an average test rate of 80 cases/second.

The accuracies of the proposed AMC obtained from the performances of ResNet18 and ResNet101 are listed in Table 2, which illustrates that the validation accuracy increases at higher SNRs and decreases at lower SNRs.

Figs. 5 and 6 compare the recognition performances in terms of accuracy versus SNR of ResNet18 and ResNet101. Fig. 5 shows that the validation accuracy of ResNet18 is
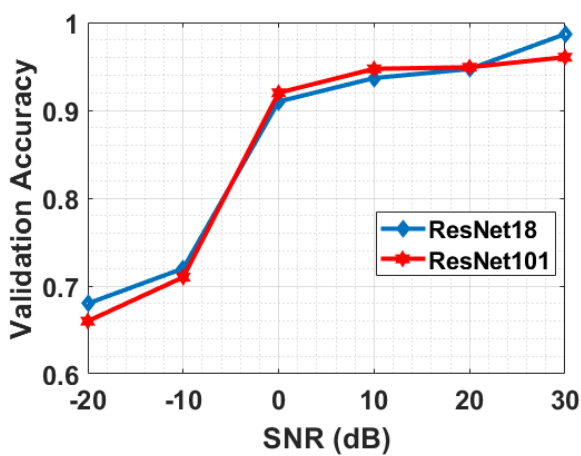
around 2.55% higher than that of ResNet101 when the SNR is 30 dB. At various SNRs, ResNet18 achieved higher classification accuracy than ResNet101. At SNR 0 dB, ResNet101 achieved 1% higher recognition accuracy than ResNet18. Fig. 6 shows that the test accuracy of ResNet18 is around 0.8% higher than that of ResNet101 when the SNR is 30 dB. At the other SNRs, ResNet18 and ResNet101 achieved slightly different recognition accuracies. Due to the difference in the structure of the utilized CNN networks, where the ResNet101 has more layers than ResNet18, the training time will be the longest, and it can be noticed a lower accuracy was achieved.

The confusion matrix evaluates the effectiveness of an algorithm. It represents the recognition accuracy for each modulation approach. Fig. 7 presents the confusion matrices of AMC. In detail, at SNR 30 dB, the total test accuracy achieved is 99.2% and 98.4% using ResNet18 and ResNet101, respectively, where a few of 4-ASK, 32-QAM, and 512-QAM are misclassed. The misclassification increases as the SNR decreases, where the test recognition accuracy achieved at 0 dB is 90.1% and 90.5% using ResNet101 and ResNet18, respectively.

Table 3 compares previous studies on this work in terms of DL models used, the types of modulations for classification, and the maximum classification accuracy achieved. As shown in Table 2, for [10], the recognition accuracy achieved is 90%, while in comparison, our proposed AMC achieved 98.68% and 96.05%. At -10 dB, the recognition accuracy of the designed AMC exceeds 70%, while in [10], the recognition accuracy is below 70%. At SNR 10 dB, the proposed work achieved higher recognition accuracy at 93%, while in [12], the accuracy achieved at a similar SNR was 91%. From 0 to 10 dB, [13] achieved the same accuracy, while in the proposed work for the same SNR range, the accuracy increases gradually. At -10 and -20 dB in [15], the recognition accuracies achieved are below 15% and 10%, while in this work and at the same SNRs, the recognition accuracies are higher at 60% and 70%. The recognition accuracies achieved in [17] are lower at 20%, 30%, and 80% at -20, -10, and 0 dB, respectively. The recognition accuracy achieved in [18] is lower at 20%, 30%, and 90% at -20, -10, and 0 dB, respectively. The utilization of pre-trained CNN models (ResNet18 and ResNet18) that have been trained on massive and diverse datasets to recognize features and patterns of the cases, which can boost the performance after retaining and achieving higher accuracies than other proposed models LSTM and Generative Adversarial Networks (GAN) over complicated environment.

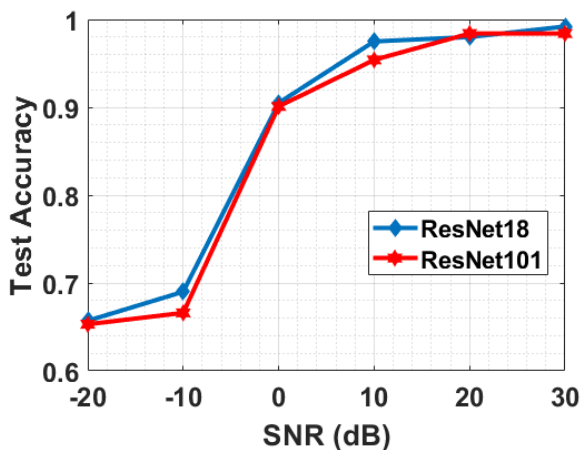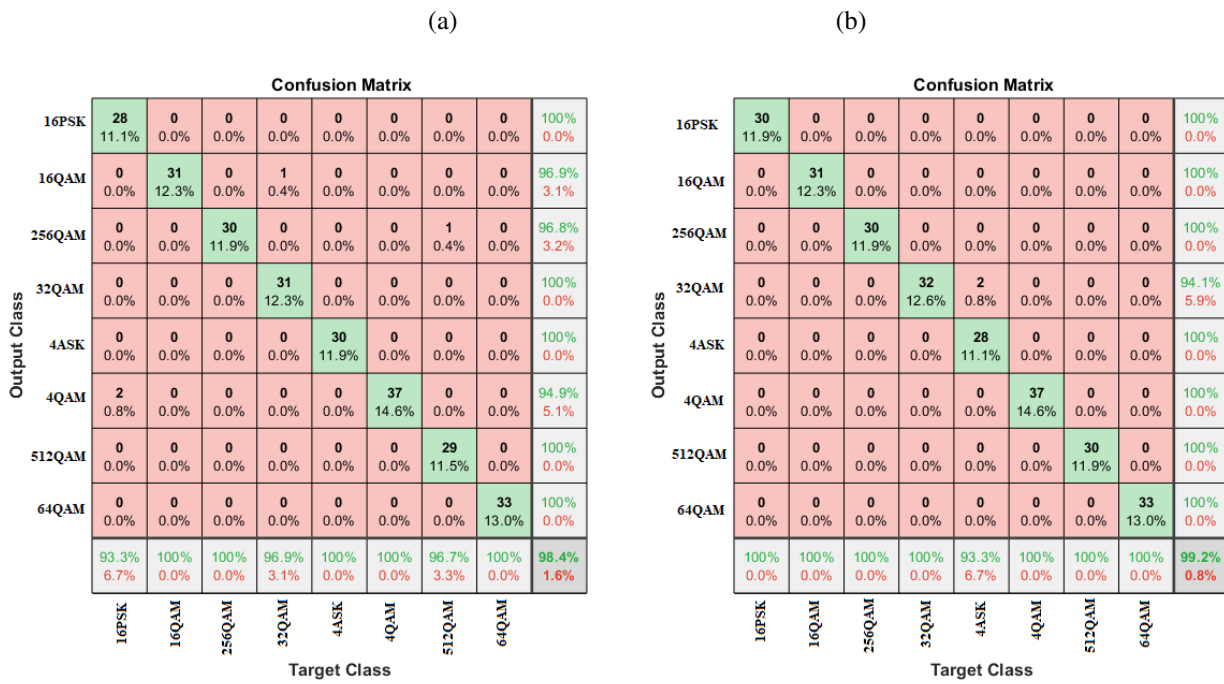**Figure 5.** Validation accuracies.

Figure 6. Test accuracies.

Table 2. Validation accuracies of resnet18 and resnet101 at various SNRs.

Model	Accuracy (-20dB)	Accuracy (-10dB)	Accuracy (0dB)	Accuracy (10dB)	Accuracy (20dB)	Accuracy (30dB)
ResNet18	68%	72%	91%	93.76%	94.7%	98.6%
ResNet101	66%	71%	92%	94.72%	94.9%	96.05%

(a)   (b)

Figure 7. Confusion Matrices of (a) ResNet101 (30dB), (b) ResNet18 (30dB).

Table 3. Comparisons with previously studied literature models.

Reference	Year	Model	Modulation Types Used	Max Accuracy (%)
[10]	2020	CNN	Binary phase shift keying (BPSK), QPSK, 8-PSK, 16-QAM	98
[12]	2022	LSTM-CNN	BPSK, QPSK, 8-PSK, BFSK, CPFSK, 4-PAM, 16-QAM, 64-QAM	98
[13]	2023	SCFNet	4-ASK, 2-PSK, 4-PSK, 8-PSK, 16-QAM, 32-QAM, 64-QAM, 128-QAM	90 to 95
[14]	2023	DenseNet-22	BPSK, CW, LFM_PULSE, , PAM, SINFM, TRIFM	90
[15]	2023	SemiAMC DL	AM-SSB, AM-DSB, BPSK, QPSK, 8-PSK, CPFSK, GFSK, 4-PAM, 16-QAM, 64-QAM, WBFM	41.6 at SNR -4 dB
[16]	2023	CNN (MobileNet-V2, ResNet 50, ResNet 18)	4-PAM,BPSK,QPSK, OQPSK, 8-PSK,16-PSK,64-PSK,16-QAM,	94.64, 92.86, and 96.43
[17]	2022	MSNet	BPSK, QPSK, 8-PSK, 16-QAM, 64-QAM, GFSK, CPFSK, 4-PAM,	90.26
[18]	2023	TDRNN	AM-SSB, AM-DSB, BPSK, QPSK, 8-PSK, CPFSK, GFSK, 16-QAM, 64-QAM, 4-PAM, WBFM	63.5
[19]	2023	KD-GSENET	16-QAM,32-QAM,64-QAM, BPSK, , QPSK, OQPSK 8-PSK, 4-ASK	100
[20]	2024	ConvLSTM and transformer block NN	AM-SSB, AM-DSB, BPSK, QPSK, 8-PSK, CPFSK, 4-PAM, 16-QAM, 64-QAM, WBFM	93.5
[21]	2024	Meta-Transformer	AM-DSB-WC, AM-SSB-WC, AM-DSB-SC, AM-SSB-SC, 4-ASK, 8-ASK, BPSK, QPSK,, OQPSK, 8-PSK, 16-PSK, 32-PSK, 16-APSK, 32-APSK, 128-APSK, 16-QAM, 32-QAM, 64-QAM, 128-QAM, 256-QAM, FM, GMSK, OOK	90
[22]	2024	two CNN models	AM-SSB, AM-DSB, BPSK, 2-PSK, QPSK, 8-PSK, 16-PSK, CPFSK, GFSK, 4-PAM, 8-QAM, 16-QAM, 64-QAM, 32-QAM, WBFM	53.65 and 94.39
This work	2024	CNN (ResNet18, ResNet101)	4-ASK,16-PSK, 4-QAM, 16-QAM, 32-QAM, 64-QAM,256-QAM, 512-QAM	98.68 and 96.05

5. Conclusion

This study introduces an AMC model designed to align with the standards of 6G communication networks. The approach comprises two main stages. In the first stage, a range of transceivers with different modulators was created. This allowed the collection of received constellation point signals, which were then compiled into a dataset and prepared for training. The second stage involved training this dataset using pre-trained CNN models. The key achievement of this research lies in the model's ability to identify modulation types under various CFO, PN, and SNR conditions. By employing two types of pre-trained CNNs, the proposed models achieved impressive recognition accuracies. Specifically, using ResNet18 and ResNet101, the models attained recognition accuracies of 98.68% and 96.05%, respectively. These high percentages effectively meet the evolving needs of advanced 6G communication networks.

Supplementary Table: Abbreviations

6G	Sixth-Generation
AMC	Automatic Modulation Classification
AM-DSB	Amplitude Modulation-Double Side Band
AM-SSB	Amplitude Modulation-Single Side Band
ASK	Amplitude Shift Keying
BFSK	Binary Frequency Shift Keying
BPSK	Binary Phase Shift Keying
CNN	Convolutional Neural Network
CFO	Carrier Frequency Offset
CPFSK	Continuous-Phase Frequency Shift Keying
CW	Continuous Wave
DL	Deep Learning
DR2D	Data Rearrangement and the 2D
FM	Frequency Modulation
GAN	Generative Adversarial Networks
GFSK	Gaussian Frequency Shift Keying
GMSK	Gaussian Minimum Shift Keying
GRU	Gated Recurrent Unit
IQ	In phase /Quadrature
LFM-PULSE	Linear Frequency Modulation Pulsing
LSTM	Long-Short Term Memory
MSNet	Mass Spectra Network
OFDM	Orthogonal Frequency Division Multiplexing
OOK	On Off Keying
OQPSK	Offset Quadrature Phase Shift Keying
PAM	Pulse Amplitude Modulation
PO	Phase Offset
PN	Phase Noise
PSK	Phase Shift Keying
QAM	Quadrature Amplitude Modulation
QPSK	Quadrature Phase Shift Keying
SCFNet	Semantic Correction and Focusing Network
SINFM	Sine wave Frequency Modulation
SNR	Signal-to-Noise Ratio
TDRNN	Time-Delay Recurrent Neural Network
TRIM	Triangle wave Frequency Modulation
WBFM	Wide Band Frequency Modulation

Authors contributions
All authors have contributed equally to prepare the paper.

Availability of data and materials
Data underlying the results presented in this paper are available from the corresponding author upon reasonable request.

Conflict of interests
The authors declare that they have no known competing financial interests or personal relationships that could have appeared to influence the work reported in this paper.

References

[1] A. Halamandaris. "**Performance Analysis of 6G Communication Links in the Presence of Phase Noise**". *Ph.D. dissertation, California State Univ., Northridge*, 2023. DOI: https://doi.org/10.1109/LATINCOM59467.2023.10361876.

[2] W. Xiao, Z. Luo, and Q. Hu. "**A Review of Research on Signal Modulation Recognition Based on Deep Learning, Electronics**". 11:2764, 2022. DOI: https://doi.org/10.3390/electronics11172764.

[3] A. Abushattal, S.E. Zegrar, A. Yazgan, and H. Arslan. "**A Comprehensive Experimental Emulation for OTFS Waveform RF-Impairments**". *Sensors*, 23:38, 2022. DOI: https://doi.org/10.3390/s23010038.

[4] O.H. Salim, A.A. Nasir, H. Mehrpouyan, W. Xiang, S. Durrani, and R.A. Kennedy. *"Channel, Phase Noise, and Frequency Offset in OFDM Systems: Joint Estimation, Data Detection, and Hybrid Cramér-Rao Lower Bound"*, volume 62. 2014. DOI: https://doi.org/10.1109/TCOMM.2014.2345056.

[5] D.M. Ali, Z.Z. Yahya, and Y.M. Abbosh. *"OTFS Waveform Effectiveness in 6G Communication Networks"*, volume 18. 2023. DOI: https://doi.org/10.46581/IJMOT20229272427.

[6] R.N. Ipanov, A.A. Komarov, and A.P. Klimova. *"Phase-Code Shift Keyed Probing Signals with Discrete Linear Frequency Shift Keying and Zero Autocorrelation Zone"*. 2019. DOI: https://doi.org/10.1109/EnT47717.2019.9030566.

[7] N. Bereczki and V. Simon. "**Machine Learning Use-Cases in C-ITS Applications**". *Infocommunications J.*, 15:26–43, 2023. DOI: https://doi.org/10.36244/icj.2023.1.4.

[8] T. O'Shea and N. West. "**Radio Machine Learning Dataset Generation with GNU Radio**". *in proc. Of the GNU Radio Conf.*, pages 1–6. URL https://pubs.gnuradio.org/index.php/grcon/article/view/11.

[9] T.J. O'Shea, T. Roy, and T.C. Clancy. "**Over-the-Air Deep Learning Based Radio Signal Classification**". *IEEE J. of Selected Topics in Signal Proc.*, 12:168–179, 2018. DOI: https://doi.org/10.1109/JSTSP.2018.2797022.

[10] J. Shi, S. Hong, C. Cai, Y. Wang, H. Huang, and G. Gui. "**Deep Learning-Based Automatic Modulation Recognition Method in the Presence of Phase Offset**". *IEEE Access*, 8:42841–42847, 2020. DOI: https://doi.org/10.1109/ACCESS.2020.2978094.

[11] H. Zhang, F. Zhou, Q. Wu, W. Wu, and R.Q. Hu. "**A Novel Automatic Modulation Classification Scheme Based on Multi-Scale Networks**". *IEEE Transactions on Cognitive Communications and Networking*, 8:97–110, 2022. DOI: https://doi.org/10.1109/TCCN.2021.3091730.

[12] M.M. Elsagheer and S.M. Ramzy. "**A hybrid model for automatic modulation classification based on residual neural networks and long short term memory**". *Alexandria Engineering J.*, 67:117–128, 2023. DOI: https://doi.org/10.1016/j.aej.2022.08.019.

[13] H. Han et al. "**Automatic Modulation Recognition Based on Deep-Learning Features Fusion of Signal and Constellation Diagram**". *Electronics*, 12:552, 2023. DOI: https://doi.org/10.3390/electronics12030552.

[14] Y. Liu, X. Yan, X. Hao, G. Yi, and D. Huang. "**Automatic Modulation Recognition of Radiation Source Signals Based on Data Rearrangement and the 2D FFT**". *Remote Sensing*, 15:518, 2023. DOI: https://doi.org/10.3390/rs15020518.

[15] Q. Zhou, R. Zhang, Z. Jing, and X. Jing. "**Semi-supervised-based automatic modulation classification with domain adaptation for wireless IoT spectrum monitoring**". *Frontiers in Physics*, 11:1158577, 2023. DOI: https://doi.org/10.3389/fphy.2023.1158577.

[16] Z.Z. Yahya and D.M. Ali. "**Software Defined Radio (SDR) Signals Classification via Convolutional Neural Networks**". *Int. J. of Microwave and Opt. Technol.*, 18:607–616, 2023. DOI: https://doi.org/10.46581/IJMOT20238352587.

[17] C. Roy et al. "**An Ensemble Deep Learning Model for Automatic Modulation Classification in 5G and Beyond IoT Networks**". *Computational Intelligence and Neuroscience*, 2021, 2021. DOI: https://doi.org/10.1155/2021/5047355.

[18] T.T. An, A.A. Puspitasari, and B.M. Lee. "**Efficient Automatic Modulation Classification for Next Generation Wireless Networks**". *TechRxiv*, pages 1–12, 2023. DOI: https://doi.org/10.36227/techrxiv.23632308.v1.

[19] L. Guo, R. Gao, Y. Cong, and L. Yang. "**Robust automatic modulation classification under noise mismatch**". *EURASIP J. on Advances in Signal Proc.*, 2023:73, 2023. DOI: https://doi.org/10.1186/s13634-023-01036-9.

[20] Z. Elkhatib, F. Kamalov, S. Moussa, A.B. Mnaouer, M. Yagoub, and H. Yanikomeroglu. "**Radio Modulation Classification Optimization Using Combinatorial Deep Learning Technique**". *IEEE Access*, 12:17552–17570, 2024. DOI: https://doi.org/10.1186/s13634-023-01036-9.

[21] J. Jang, J. Pyo, Y.-I. Yoon, and J. Choi. "**Meta-Transformer, A Meta-Learning Framework for Scalable Automatic Modulation Classification**". *IEEE Access*, 12:9267–9276, 2024. DOI: https://doi.org/10.1109/ACCESS.2024.3352634.

[22] S. Mohsen, A.M. Ali, and A. Emam. "**Automatic modulation recognition using CNN deep learning models**". *Multimedia Tools and App.*, 83:7035–56, 2024. DOI: https://doi.org/10.1007/s11042-023-15814-y.